Journal of Organometallic Chemistry 693 (2008) 2111–2118

Contents lists available at ScienceDirect

Journal of Organometallic Chemistry

journal homepage: www.elsevier.com/locate/jorganchem

Structural evolution of a recoverable rhodium hydrogenation catalyst

Wendy J. Shaw [a,*], Yongsheng Chen [d], John Fulton [a], John Linehan [a], Anna Gutowska [c], Tom Bitterwolf [b]

[a] Chemical Sciences Division, Pacific Northwest National Laboratory, Richland, WA 99352, United States
[b] University of Idaho, Moscow, ID, United States
[c] Advanced Imaging Technology, Richland, WA, United States
[d] Pennsylvania State University, University Park, PA 16802, United States

ARTICLE INFO

Article history:
Received 29 January 2008
Received in revised form 7 March 2008
Accepted 8 March 2008
Available online 15 March 2008

Keywords:
Homogeneous catalysis
Aqueous rhodium catalysts
Stimulus sensitive polymers
Recoverable catalyst
High pressure NMR

ABSTRACT

A recoverable, water soluble, hydrogenation catalyst was synthesized by reacting poly-*N*-isopropylacrylamide containing a terminal amino group ($H_2N–CH_2CH_2–S–$pNIPAAm) with $[Rh(CO)_2Cl]_2$ in organic solvents to form the square planar rhodium complex ($Rh(CO)_2Cl(H_2$**N**$–CH_2CH_2–S–$pNIPAAm)). The catalyst–ligand structure was characterized using *in situ* multinuclear NMR, XAFS and IR spectroscopic methods. Model complexes containing glycine (H_2NCH_2COOH), cysteamine ($H_2NCH_2CH_2SH$) and methionine methyl ester ($H_2NCH(CH_2CH_2SCH_3)COOCH_3$) ligands were studied to aid in the interpretation of the coordination sphere of the rhodium catalyst. The spectroscopic data revealed a switch in ligation from the amine bound ($Rh–NH_2–CH_2CH_2–S–$pNIPAAm) to the thioether bound ($Rh–S(–CH_2CH_2NH_2)(–$pNIPAAm)) rhodium when the complex was dissolved in water. The evolution of the structure of the rhodium complex dissolved in water was followed by XAFS. The structure changed from the expected monomeric complex to form a rhodium cluster of up to four rhodium atoms containing one SRR′ ligand and one CO ligand per rhodium center. No metallic rhodium was observed during this transformation. The rhodium–rhodium interactions were disrupted when an alkene (3-butenol) was added to the aqueous solution. The kinetics of the hydrogenation reaction were measured using a novel high-pressure flow-through NMR system and the catalyst was found to have a TOF of 3000/Rh/h at 25 °C for the hydrogenation of 3-butenol in water.

Published by Elsevier B.V.

1. Introduction

Coupling the reactivity and selectivity of homogenous catalysts with the robustness and recoverability of heterogeneous catalysts is a significant goal in transition-metal catalysis. One approach is the immobilization of homogenous catalysts through complexation to polymers or surfaces. Recently, investigations were initiated into a new, direct synthetic route for attaching a rhodium catalyst onto poly-*N*-isopropylacrylamide (pNIPAAm) [1]. The pNIPAAm polymer exhibits inverse temperature solubility in water [2]. Inverse temperature solubility (insoluble at higher temperatures while soluble at lower temperatures) results in the precipitation of the polymer as the temperature increases and results in a remarkable capacity for recovery [3,4]. The resulting recoverable catalyst showed promise for hydrogenation applications [1]. While other studies have been pursued with polymers as soluble supports [5–8], typically the polymer is viewed as only a support and not involved as an integral part of the catalyst. Thus, limited structural characterization has been performed on the catalysts attached to these polymers. This study expands upon the initial studies of this recoverable hydrogenation catalyst utilizing *in situ* XAFS, NMR and IR spectroscopic methods along with the characterization of model rhodium complexes to further elucidate the catalyst structure.

As a macromolecular ligand that is also a soluble support, pNIPAAm has several advantages for catalysts. pNIPAAm is soluble in many solvents, can be synthesized reproducibly at many different molecular weights and a variety of functional groups can easily be incorporated. Perhaps most important for catalyst recovery is the property of inverse solubility. Termed the lowest critical solution temperature, or LCST, this very sharp phase transition in water is due to the change in hydrophobic vs. hydrophilic interactions, and can be predictably controlled by changing polymer length or incorporating copolymer adducts [2,9]. The pNIPAAm utilized in this study (4400–16000 a.m.u.) exhibits an LCST of ~33 °C, which facilitates low temperature catalyst recovery.

The rhodium catalyst was attached to pNIPAAm through the amine terminal linker in THF as previously reported (Scheme 1) [1,10]. The static structure of the solid Rh–pNIPAAm characterized by FTIR, Raman, and XAFS [1] spectroscopies is consistent with the product structure shown in Scheme 1. However, the structure of a catalyst, or catalyst precursor, in the solid state can be quite different than the catalyst in solution. *In situ* methods allow the investigation of the rhodium complex under conditions found during

* Corresponding author.
E-mail address: wendy.shaw@pnl.gov (W.J. Shaw).

0022-328X/$ - see front matter Published by Elsevier B.V.
doi:10.1016/j.jorganchem.2008.03.011

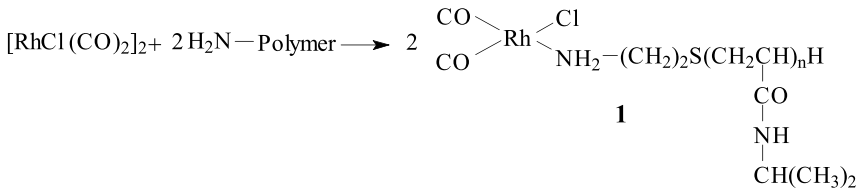

Scheme 1. Reaction to form stimulus sensitive catalyst precursor.

catalysis (i.e., solvent, temperature, pressure), revealing important structural information that might otherwise be unobserved.

The ligand structure about the rhodium could not be analyzed by X-ray crystallography since we were unable to obtain single crystals. Three different spectroscopic methods (XAFS, NMR and IR) were employed to evaluate the structure of this compound. NMR is capable of providing details of the ligands bound to the rhodium both by chemical shift and by coupling constants and the NMR method can be enhanced by the use of isotopic labeling. XAFS is well suited to resolving the first-shell structure about the rhodium center including specific information about coordination number, bond distance and disorder. A limitation is that it is not possible to fully resolve atoms that differ by only one or two atomic numbers (ie N vs. O) based on XAFS alone. As an additional confirmation of the structure, the binding of chemically simple analogs was examined to understand the ligand environment about the Rh–pNIPAAm complex. Combined with complimentary NMR techniques, it is possible to completely resolve the first-shell structure. This work investigates the dynamic structure of this recoverable catalyst, first in water, then in the presence of the reactants (3-buten-1-ol and H_2) used for hydrogenation kinetics.

2. Experimental

2.1. Materials

N-isopropylacrylamide (NIPAAm) (Acros Organics) was recrystallized from *n*-hexane and dried under vacuum. 2,2′-Azobisisobutyronitrile (AIBN) (98%, Aldrich) was recrystallized from methanol before use. Cysteamine was purchased from Sigma and used as received. *N*,*N*-Dimethylformamide, (HPLC grade, Aldrich), diethyl ether and hexane (reagent grade, Aldrich) and deuterated solvents (Aldrich) were used as received. Unlabeled $[Rh(CO)_2(Cl)]_2$ was purchased from Strem and used as received.

2.2. Synthesis of amino-terminated oligo(N-isopropylacrylamide)(oligo(NIPA)-NH_2)

Oligomers of *N*-isopropylacrylamide (NIPAAm) with a single terminal amine group were synthesized by free-radical polymerization using AIBN as an initiator and cysteamine as a chain transfer agent. Specifically, 10 g of NIPAAm was dissolved in 37.4 mL of DMF, and 68.4 mg of cysteamine along with 111.9 mg of AIBN were added. The solution was deoxygenated with nitrogen for 1 h before heating to 70 °C and stirring in an inert atmosphere for 18 h. After partial evaporation of DMF, the products were precipitated with a 10-fold excess of diethyl ether and separated by filtration. The crude oligomers were dried under vacuum, dissolved in 350 mL of 18 MΩ H_2O, and purified by ultrafiltration using a 1000 D molecular weight cut-off membrane. Purified oligomers were recovered from water by freeze-drying. The average molecular weight of the oligomers was determined by end-group titration with bromophenol blue by dissolving 80 mg of the polymer in 20 mL of water and titrating to the yellow endpoint with an aqueous solution of 0.0200 N HCl. One preparation resulted in a 4400 a.m.u polymer and one preparation resulted in a 16000 a.m.u. polymer.

2.3. Synthesis of $[Rh(^{13}CO)_2(Cl)]_2$

^{13}CO labeled $[Rh(CO)_2(Cl)]_2$ was prepared as follows: $[Rh(CO)_2Cl]_2$, 100 mg, 0.25 mmol, was dissolved in 30 mL of dry, air-free petroleum ether under N_2 and transferred by syringe to a N_2 flushed Kontes 60 mL quartz Griffin–Worden tube. The pressure head was fitted to the tube and the completed apparatus was connected to a brass manifold with a pressure gauge, connections to a vacuum line and a laboratory cylinder containing ^{13}CO (Cambridge Isotopes, Inc. 99% ^{13}C). The Griffin–Worden tube was immersed in LN_2 to freeze the solution, then the tube and manifold were evacuated. ^{13}CO was back filled into the tube to atmospheric pressure. The tube was photolyzed for 3 h using a 350 W high-pressure mercury lamp, then reattached to the manifold. The tube was frozen and evacuated, and a second charge of ^{13}CO was introduced. Following three repetitions of this sequence, IR showed the rhodium carbonyl chloride dimer to be >95% transformed to the ^{13}CO isotopomer. The compound may be purified by sublimation, although here it was used without further purification.

2.4. Synthesis of $[Rh(CO)_2(Br)]_2$

The compound was prepared according to the procedure of Hieber and Lagally [11] for the analogous chloride derivative. IR is consistent with literature reports [12].

2.5. Synthesis of Rh–pNIPAAm catalyst

The Rh–pNIPAAm catalyst ($Rh(CO)_2(Cl)$(pNIPAAm)) (**1**) was prepared under inert atmosphere by adding 1/2 mol equivalent $[Rh(CO)_2(Cl)]_2$ in THF to 1 mol equivalent of 4400 D pNIPAAm polymer in THF. The mixing of the two solutions caused a slight color change from intense yellow-orange to light yellow. The solvent was removed and the catalyst was stored under nitrogen as a solid until used. For the XAFS comparison of the Cl and Br ligands only, 16000 D polymer was used.

2.6. Model catalyst preparation

The model catalysts were prepared under inert atmosphere in NMR tubes by adding 1/2 mol equivalent $[Rh(CO)_2(Cl)]_2$ in THF to 1 mol equivalent model compound in D_2O to yield a resulting concentration of 0.068 M rhodium complex in a 50% THF/D_2O mixture. The tubes were sealed with septa and parafilm to maintain the N_2 atmosphere. Three complexes (Rh-Glycine, Rh-methionine methyl ester and Rh-cysteamine) were investigated by both NMR and XAFS. Samples were investigated by NMR on day 1 and day 39 (before and after XAFS experiments) to look for any changes in catalyst structure over time. XAFS measurements were taken on day 8.

2.7. NMR

NMR experiments were performed on either a 7.06 or 11.75 T (300 and 500 MHz ^1H frequency, respectively) instrument with Varian consoles and probes. Rh–pNIPAAm structural characterization was undertaken at a concentration of 0.004 M in acetonitrile-

d_3, D_2O and mixtures of the two solvents. Model complexes were 0.068 M in 50% THF/D_2O.

2.8. Catalysis

Flow through NMR experiments were performed at (20 °C) and utilized a standard Varian 2 channel probe, modified with 1/16 in. PEEK tubing inserted vertically through the probe, replacing the sample tube. This was connected to a high-pressure cell and a Flow Solutions micropump to achieve complete mixing. Solutions were evacuated to <100 mTorr prior to the introduction of 500 psi H_2. The catalyst concentration was 2.6×10^{-4} M, with a substrate (3-buten-1-ol) concentration of 0.46 M in D_2O. Reaction solutions were mixed constantly, except during spectral acquisition.

2.9. FTIR

IR experiments were performed with a Nicolet Nexus 870 FTIR. KBr pellets or thin films between ZnSe windows in water, THF or MeCN were investigated.

2.10. XAFS

The rhodium K-edge (23 222 eV) XAFS spectra were collected in transmission mode on the bending magnet beamline (PNC-CAT, Sector 20) at the Advanced Photon Source, Argonne National Laboratory. All spectra were acquired in transmission mode using a variety of different sample holders. For dilute rhodium polymer samples in water, a pathlength of 5 cm was used. Sample cells consisted of either a 5 mL, sealed silica sample bottle or a high-pressure, 316 SS vessel with PEEK X-ray windows for the hydrogenation reactions. The high-pressure reactor used for these *in situ* XAFS studies was constructed from a standard high-pressure fitting (part # 20-23LF9, High Pressure Equipment, Erie, PA). The two standard end plugs used in this fitting were replaced by modified PEEK inserts to provide the X-ray beam transmission. A high-speed, micro stir bar, placed just below the gas–liquid interface, ensured that the liquid phase was saturated by H_2 throughout the course of the reaction. The H_2 gas was supplied to the reactor from a fixed-volume reservoir that was initially filled from a standard lecture bottle. The solution was vigorously stirred during the hydrogenation reaction. The rhodium-model compound catalysts were contained in sealed NMR tubes (5 mm OD × 4.25 mm ID), see sample prep above. Beam size was typically 1 × 5 mm with a total flux of approximately 8×10^9 photons/s. Harmonic rejection was accomplished through 20% detuning of the monochromator crystal.

The fitting of the FEFF8 theoretical standards [13] to the experimental XAFS spectra was accomplished using the IFEFFIT analysis program [14,15]. Several examples of quality of fits for various samples and standards are reported in the Supplementary Material and yield coordination numbers of ±20%. XAFS sample concentrations were: 4.3 mM for Rh–pNIPAAm, 1 mM for the comparison of $Rh(CO)_2(Cl)$(pNIPAAm) and $Rh(CO)_2(Br)$(pNIPAAm), and 68 mM for the amino acid derivative catalysts.

3. Results and discussion

3.1. NMR structural studies

The $^{13}C\{^1H\}$ NMR of the ^{13}CO–Rh–pNIPAAm catalyst precursor, **1**, dissolved in d_8-THF exhibits a very broad peak, compared to the doublet (δ 178.9, J^1(Rh–C) = 76 Hz) observed for $[Rh(CO)_2(Cl)]_2$ (data not shown). In acetonitrile-d_3, the broad peak (δ 182.4) was coincident with a very sharp doublet (δ 182.3, J^1(Rh–C) = 71 Hz), indicating at least two types of COs, one that is apparently exchangeable (broad) and one that is less labile (narrow doublet) (Fig. 1b, Table 1). There was no change in this spectrum after 5 days. The release of CO_2 (125–126 ppm) from **1** is also observed

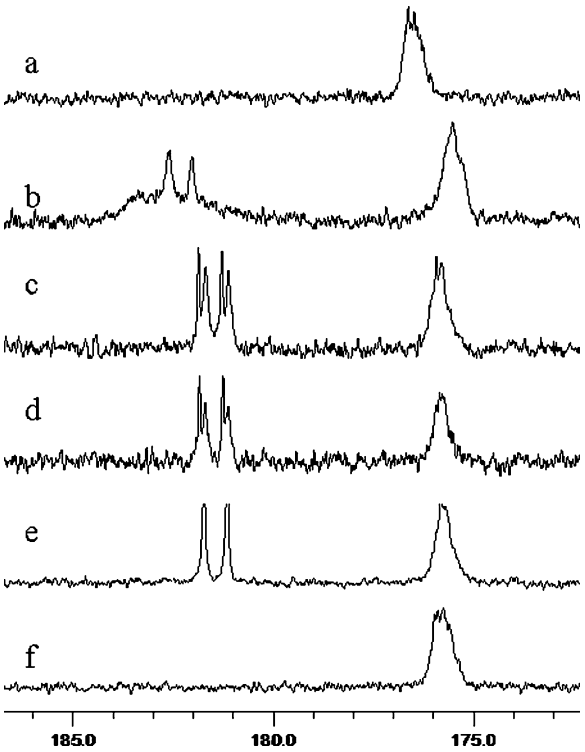

Fig. 1. ^{13}C NMR spectra of Rh–pNIPAAm catalysts. From top to bottom: (a) pNIPAAm in D_2O. (b) **1** (prepared with isotopically labeled ^{13}COs) in acetonitrile-d_3 immediately after dissolution, (c) sample b immediately upon the addition of 25% D_2O, (d) sample c 1 h after D_2O addition, (e) sample c 20 h after D_2O addition, (f) **1** in 100% D_2O. The series shows the eventual loss of CO (180–185 ppm) with additional exposure to water.

Table 1
^{13}C carbonyl chemical shifts for starting and product materials as a function of preparation

Compound	Chemical shift(s) ppm(±0.1)	Coupling (Hz)(±1)
$[Rh(CO)_2(Cl)]_2$ (THF)	178.9 (d)	76
$[Rh(CO)_2(Cl)]_2$	181.2 (d)	62
1 in acetonitrile	182.3 (d)	71
	182.4 (broad)	–
1 in 25% H_2O/MeCN	181.4 (d)	71
	181.6 (d)	73
1 in 25% H_2O/MeCN, 20 h later	181.4 (d)	72
1 in 100% H_2O	–	–
Rh-cysteamine	181.5 (d)	68
	182.2	–
	183.5 (d)	70
	186.4 (d)	65
Rh-cysteamine[a]	183.2 (d)	70
Rh-methionine	181.3 (d)	72
Rh-methionine[a]	180.3 (d)	72
	183.0 (d)	76
Rh-glycine	181.6 (d)	56
	183.2 (q)	56 ± 5
Rh-glycine[a]	–	–

Samples were dissolved in 50% THF/D_2O unless otherwise indicated.
[a] After 39 days.

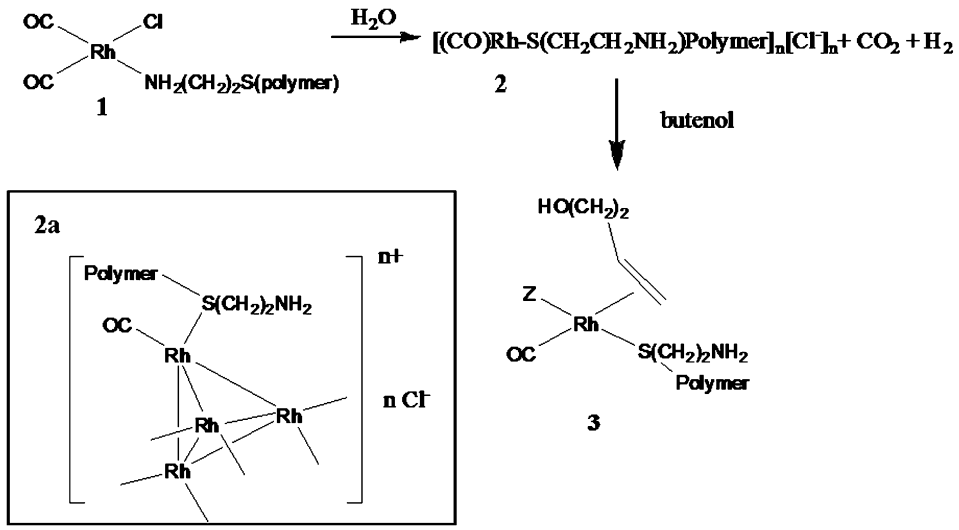

Fig. 2. Proposed structures based on spectroscopic analysis of rhodium pNIPAAm complexes. Any potential rhodium hydride ligands (perhaps Z in structure **3**) are not observed by proton NMR and are not observable by XAFS. The inset in **2a** is a possible configuration of **2**, consistent with the available data, where the ligands are only shown on one-Rh center for clarity, and represented by lines on each of the other Rh centers in the cluster.

within the preparation time of the samples (on the order of 30 min) in both THF and acetonitrile solvents indicative of a water-gas shift reaction converting CO to CO_2. The water source is most likely residual water from the lyophilized polymer which could not be completely dried.

Based on the following NMR observations, **1** undergoes a ligand reconfiguration in water with the loss of one carbonyl in 50% water, and the loss of both carbonyl ligands and/or rapid CO exchange in pure water. Two doublets (δ 181.6, J^1(Rh–C) = 73 Hz, δ 181.4, J^1(Rh–C) = 71 Hz) are observed after the addition of enough D_2O to yield a 25% solution, suggesting the presence of two different rhodium carbonyl species (Fig. 1c), the broad upfield doublet (linewidth = 20 Hz vs. 7 Hz) suggests possible exchange. Within an hour, the upfield peak was broadened (Fig. 1d), and 20 h after the addition of D_2O resulted in the loss of the downfield CO species (δ 181.6 ppm), and a reduction in linewidth of the upfield CO (δ 181.4 ppm) to 13 Hz, with a J^1(Rh–C) = 72 Hz (Fig. 1e). Adding additional D_2O to yield a 50% D_2O solution resulted in little change to the spectrum (δ 181.2 ppm, J^1(Rh–C) = 73 Hz) (data not shown). No carbonyl resonances were observed when solid **1** was dissolved in D_2O (0.01 M) without an organic co-solvent (Fig. 1f), due to complete CO loss, or CO exchange on the NMR timescale. This result is consistent with FTIR observations in which no carbonyl bands were observed in pure water and the carbonyl band intensity (2080, 2010 cm^{-1}) slowly decreased with increasing percentages of water in acetonitrile (at 15% water/acetonitrile no carbonyl signal could be detected). The carbonyl stretches are observable by FTIR in up to a 50% H_2O/THF mixture. In summary, utilizing labeled ^{13}CO ligands, NMR and IR measurements suggest that **1** undergoes a ligand reconfiguration in water, including the loss of one carbonyl in 50% water, and the loss of both carbonyl ligands and/or rapid CO exchange in pure water. The available NMR spectroscopic evidence did not provide insight into what replaced the CO ligands.

3.2. XAFS structural studies

To further investigate the dynamic structure of **1**, XAFS experiments, complementary to the NMR experimental studies, were undertaken to directly investigate the ligands attached to the rhodium center Not only can XAFS determine the identity and coordination number of attached ligands, it is also possible with XAFS to clearly differentiate a nearest neighbor Cl from that of a C or O (and likewise other atoms that reside in different rows in the periodic table).

The structure of solid **1** determined by XAFS is consistent with that shown in Scheme 1 and Fig. 2(**1**), as previously reported [1]. However, in water **1** undergoes an unexpected dramatic ligand rearrangement including the substitution of the thioether sulfur for the amine.[1] At early times, within 24 h, XAFS data (Fig. 3 and Table 2) of 4.3 mM **1** dissolved in water (red line) are modeled with a species containing two carbonyls, one sulfur, one nitrogen and one rhodium (Table 2), the sulfur ligand and the Rh–Rh interaction being a significant departure from the solid state structure. Thirty-three hours later (57 h after preparation), the nitrogen ligand and one of the carbonyl ligands were lost, and the XAFS data are consistent with the formation of a tetrameric rhodium cluster (see Fig. 2, Table 2), with one CO and one sulfur ligand per rhodium center remaining. Fig. 2a is the most probable structural configuration consistent with the XAFS data. The large Rh–Rh coordination number (1.7) (Table 2) when initially dissolved in water is likely a combination of several structures involving 1–4 Rh atoms in equilibrium. The presence of rhodium metal from colloidal Rh was not observed based on the absence of third and higher Rh–Rh shells in the XAFS analysis.

3.3. Model compound studies

The structures predicted by XAFS and NMR data of the aqueous soluble catalyst were markedly different than the solid catalyst and warranted further investigation to confirm a radical change in first-shell ligand identity. We approached this by examining model compounds and a variety of spectroscopic techniques to confirm each of the proposed ligands of the aqueous soluble catalyst: CO, S, Cl, N and Rh.

Carbonyl ligands. The initial presence of carbonyl ligands, and loss of carbonyl with time as observed by XAFS was consistent with the NMR data. Carbonyl ligands were still present in the XAFS spectrum after 2 days, even though no carbonyl was observed by NMR. This observation is rationalized by exchange broadening on

[1] The substitution of the amine by a chloride ligand is not occurring (*vida infra*). While chloride and sulfur are difficult to differentiate by XAFS, bromide and sulfur have significantly different scatterings to allow this differentiation. Very similar XAFS scattering patterns were observed in water when bromide was substituted for chloride suggesting that the halide does not displace the nitrogen.

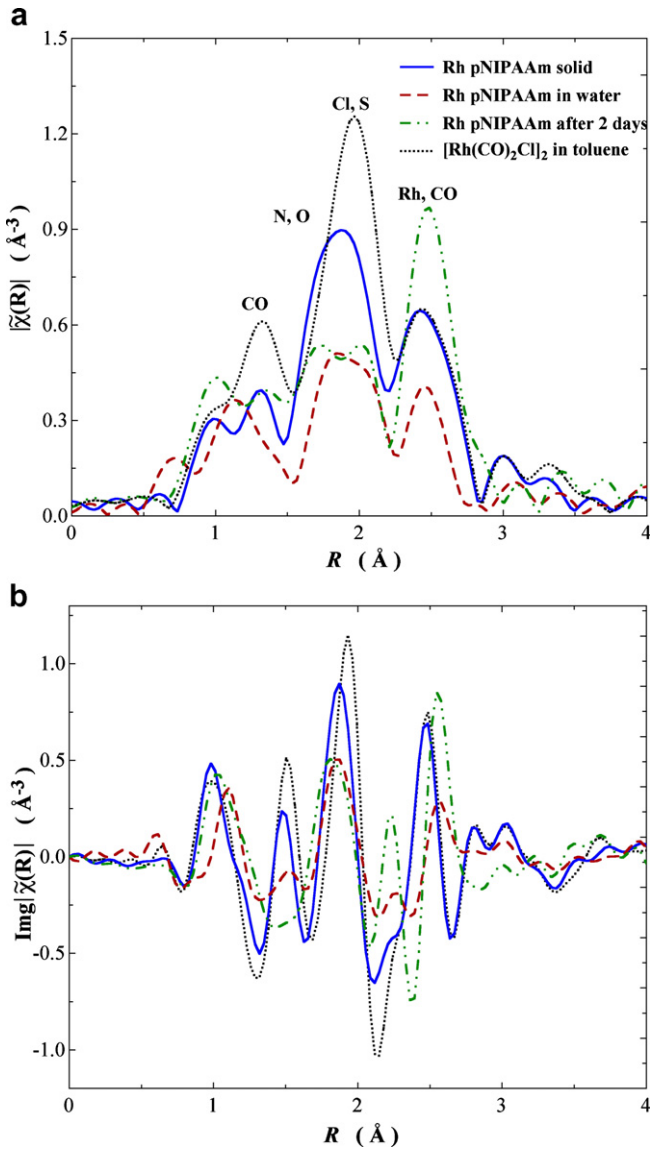

Fig. 3. The XAFS (a) radial structure plots (RSP) and (b) imaginary portion of $\tilde{\chi}(r)$ for Rh–pNIPAAm as a solid (blue), dissolved in water (red), dissolved in water after 2 days (green) and the precursor material in toluene for comparison (black). The changes in peak position and intensity indicate a change in first shell ligands. (For interpretation of the references to colour in this figure legend, the reader is referred to the web version of this article.)

the NMR timescale, as observed for metal-cluster CO ligands [16]. Further investigation by low temperature NMR experiments was not possible due to the limited temperature range of liquid water.[2]

Sulfur ligand. XAFS data show that the sulfur ligand binds when dissolved in water but not in the initial solid polymer compound. The presence of a sulfur ligand bound in aqueous conditions was further investigated. The thioether, contained within the amine linker group (Scheme 1), is well positioned to result in a five-membered ring if it is bound through both the amine and thioether. This configuration does not fit the XAFS data in the solid state or in THF, suggesting that the sulfur is in some way "activated" to bind when **1** is added to water. To test this hypothesis, methionine methyl ester and cysteamine, were ligated to Rh as models for **1**

[2] A spectrum was taken at 6 °C and no difference was seen. Investigation at higher temperatures (above 33 °C) is not possible due to the precipitation of the temperature sensitive catalyst.

Table 2
XAFS fits of the coordination about Rh for **1** as solid and in solution ([Rh] = 4.3 mM), and Rh-cysteamine and Rh-methionine methyl ester ([Rh] = 68 mM)

System	Ligand	*N*	*R* (Å)	σ^{2a}	$\Re^b$
1, solid	CO	**1.8**(0.1)	1.84(1)	2.5[d]	0.027
	Cl	**1.4**(0.3)	2.34(1)	2.9(1.8)	
	N	**1.0**[e]	2.11(1)	2.3(3.1)	
1, in H_2O	CO	**1.5**(0.2)	1.86(2)	2.5[d]	0.075
	S	**0.6**(0.3)	2.34(5)	5.0[f]	
	Rh	**1.7**(0.4)	2.72(1)	6.3[f]	
	N	**1.0**[e]	2.11(3)	3.0(4.2)	
1, in H_2O	CO	**0.3**(0.3)	1.83(2)	2.5[d]	0.116
After 2 days	S	**0.9**(0.3)	2.31	5.0[f]	
	Rh	**3.6**(1.0)	2.70(1)	7.8(1.9)	
1, in 0.7 M	CO	**0.9**(0.1)	1.83(1)	2.5[d]	0.022
butenol/H_2O	S	**1.3**(0.4)	2.37(1)	5.0(2.1)	
	Rh	**0.4**(0.2)	2.75(3)	6.3[f]	
	C=C	**1.0**(0.6)[g]	2.13(1)	1.2(1.7)	
Rh-Cys in H_2O	CO	**1.8**(0.2)	1.87(1)	2.5(0.9)	0.007
	Cl	**1.2**(0.1)	2.38(1)	1.7(0.9)	
	S	**1.2**[c]	2.31	1.9(0.7)	
	Rh	**1.6**(1.0)	2.71(4)	12.5(5.7)	
Rh-Meth in H_2O	CO	**1.8**(0.2)	1.84(1)	2.2(1.0)	0.010
	Cl	**1.1**(0.1)	2.39(1)	1.7(1.1)	
	S	**1.1**[c]	2.32	1.8(0.9)	
	Rh	**1.0**(0.6)	2.73(4)	8.5(4.3)	

[a] $\times 10^3$, Å^2.
[b] Goodness of fit defined by a scaled sum of squares.
[c] Cl:S ratio fixed at 1:1 in fitting; difference in the Cl, S distances set at 0.07 Å, see text.
[d] σ^2 for these CO paths are fixed to value for $[Rh(CO)_2Cl]_2$ standard.
[e] Model includes first-shell *N* suggested from NMR results, *N* and σ^2 were constrained to best estimates since the uncertainties were high.
[f] Estimated σ^2 from standards or as measured from other samples.
[g] Number of carbons from butenol ligand.

and investigated by both XAFS and ^{13}C NMR spectroscopy. Methionine ($H_2NCH(CH_2CH_2SCH_3)COOCH_3$) contains a thioether that could form a six membered ring, observed previously for Ru(II) compounds [17]. Cysteamine ($NH_2CH_2CH_2SH$) could form a 5 membered ring as is postulated for **1** dissolved in water, and has been observed previously for Rh(III) complexes [18,19].

The first-shell ligand structure derived from XAFS for Rh-cysteamine (50% THF/D_2O) contained approximately one-S, one-Cl, one-Rh and two-CO's (Fig. 4a, Table 2). By $^{13}C\{^1H\}$ NMR, the Rh-cysteamine initially looked more complex, with four different types of COs (Table 1).

After 39 days, ^{13}C NMR showed only one CO, consistent with the XAFS data. These observations are consistent with several Rh species initially in equilibrium. One possibility is that the cysteamine initially binds directly through the sulfur group as shown in Fig. 4a (left), rearranging to contain a Rh–Rh bond and two bridging sulfurs Fig. 4a (right) over time. In a slow rearrangement, with possible intermediates, this initial structure would result in a complex spectrum by NMR, with the NMR spectrum simplifying at later times when complete conversion to Fig. 4a (right) had occurred. Thus, for Rh-cysteamine complex, a ligand binding through the sulfur (Fig. 4a) is consistent with both the XAFS and NMR data and provides evidence that the polymer could bind through the thioether sulfur in an aqueous solvent. There is no evidence of binding through the amine, indicating that the sulfur is a stronger ligand in water, consistent with the switch from "N" to "S" observed for **1** (Fig. 2) as a function of solvent.

It should be emphasized that the terminal sulfur in cysteamine is a better ligand than the thioether found in the pNIPAAm, so a thioether, methionine methyl ester, was also investigated. Rh-methionine methyl ester exhibits a doublet by ^{13}C NMR initially, indicating either two equivalent COs or only one CO (Table 1). XAFS

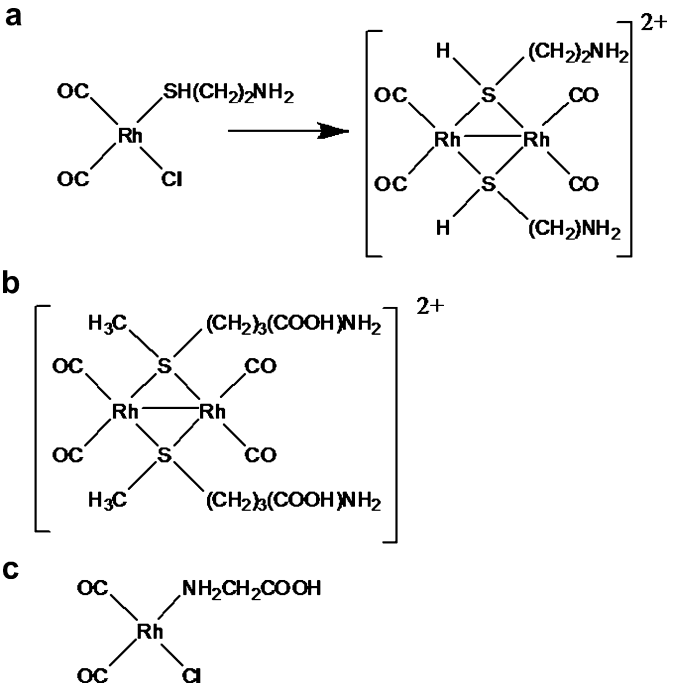

Fig. 4. Possible structures in 50% THF/H_2O as determined, by XAFS and by NMR for Rh-amine catalysts. (a) Rh-cysteamine initially (left) and with time (right), (b) Rh-methionine, and (c) Rh-glycine.

data was consistent with two equivalent COs found in a bridged structure, modeled best by one-S, one-Cl, one-Rh and two-CO ligands (Fig. 4b), similar to structures observed by others previously [20–22]. Based on the less complex NMR at early times, the thioether ligand (Rh-methionine) appears to react with rhodium and rearranges more rapidly than the terminal sulfur in cysteamine. Both of the model sulfur containing compounds support the possibility of Rh–S and Rh–Rh bonds in aqueous solvents. Neither of the model compounds contained a coordinated amine ligand. Both of the model compounds provide strong supporting evidence that the polymer–catalyst (**1**) binds through the thioether ligand and develops into rhodium clusters in aqueous solutions.

Amine ligand. To confirm binding through the amine group, a different technique was necessary due to a limitation of XAFS in distinguishing between low molecular weight atoms (nitrogen, oxygen or carbon). The solid state structure was consistent with binding through the amine group, however, the XAFS evidence in water suggests the loss of Rh–N with time. To obtain direct spectroscopic evidence, $^{15}NH_2CH_2COOH$ labeled Rh-glycine was examined by NMR and XAFS. Mixing a 2:1 mixture of the labeled glycine and $[Rh(CO)_2Cl]_2$ resulted in a product containing two inequivalent carbonyls, as would be expected for the Rh-glycine complex (Fig. 4c). $^{15}N\{^1H\}$ NMR showed a new peak ~36 ppm upfield (δ −335.7 ppm) from the starting material (−299 ppm). This is consistent with the formation of a Rh–N bond, based on the chemical shifts for other Rh–N compounds [23,24] and provides the first direct spectroscopic evidence of Rh-glycine attachment through the amine[25–28]. The observed linewidth of 45 Hz eliminated the possibility of observing the Rh–N coupling, typically on the order of 5–20 Hz[23]. To confirm that the binding was through the amine and not through the acid group of glycine, the experiment was repeated with FMOC (fluorenylmethoxycarbonyl)-protected glycine (FMOC–^{15}NH–CH_2–COOH). No reaction was observed, as expected if the binding was to the amine. When the pH of the FMOC-protected sample was adjusted to ~7, we observed a new peak in the ^{15}N NMR at 20 ppm *downfield* of the unreacted material, indicating binding through the acid group, and also confirming, based on product chemical shift, that the product peak observed for the unprotected material is not attached through the acid group.

This data confirms that binding to Rh(I) through an amine group in aqueous solvents is possible. The data also suggest that in water, the Rh–S bond is more favorable, as the best fit for the XAFS data of cysteamine and methionine methyl ester showed binding through the S and not through the N. Unfortunately, isotopically enriched cysteamine is not available to directly confirm the presence of NH_2 as a ligand in the polymer–catalyst complex. The XAFS data of the model compounds in water suggest that the NH_2 and thioether ligands of **1** rearrange when going from organic to aqueous solvents.

Chloride ligand. The XAFS data in aqueous solvents are most consistent with a loss of Cl. To further provide positive identification of the Cl ligand, we investigated the complex in two ways: by observing dissociated Cl^- using ^{35}Cl NMR and with XAFS, by preparing the catalyst using rhodium carbonyl bromide as the precursor. ^{35}Cl NMR experiments provide a unique opportunity for characterizing the Cl^- ligand. Because of the quadrupolar nature of the nucleus (spin = 3/2), asymmetric centers are not observed by solution ^{35}Cl NMR, therefore, only dissociated Cl^- will be observable by NMR. For a solution of 5–12 mM Rh–pNIPAAm, we observed Cl^- in solution, indicating that the Cl was dissociating from the complex. By way of comparison, $[RhCl(CO)_2]_2$ in d_8-THF was also examined at similar and higher concentrations and no ^{35}Cl signal was observed, as expected.

The presence or absence of chlorine as a ligand was also investigated by XAFS, by replacing the chloride with bromide in the precursor material. This was necessary because XAFS spectroscopy is unable to positively distinguish sulfur from chlorine. Bromine exhibits a different signature than chlorine in the XAFS spectrum, since the Rh–Br bond distance is slightly longer (by 0.15 Å) and the backscattering phase shift and amplitude functions are significantly different for Br vs. Cl. This data showed that the Br^- completely dissociated from the rhodium, providing a second spectroscopic method demonstrating that the chloride ligand in **1** is lost when dissolved in water. This also provides direct evidence that the chloride ligand and not the sulfur ligand is lost, confirming the presence of a sulfur ligand in the final catalyst structure.

Through the use of combined, complementary spectroscopic techniques, along with the selective investigation of model compounds, significant insight into this recoverable catalyst has been revealed. The first shell structure not only changes significantly when dissolved in water, but forms Rh clusters which could be important for catalytic activity. To further investigate this possibility, the kinetics of the catalyst in a hydrogenation reaction were measured and the XAFS structure was evaluated under similar conditions.

3.4. High pressure flow-through catalysis

The activity of the catalyst was monitored using a novel flow-through high-pressure system. This system allows for the continuous flowing of the solution, except when actually taking the NMR measurement, eliminating solvent-gas mass transfer problems (Fig. 5). As a test reaction, the hydrogenation of 3-butenol to butanol was chosen. Butenol (0.46 M) and the solid catalyst precursor ($Rh(CO)_2Cl(H_2$**N**-CH_2CH_2–S–pNIPAAm)) (2.6×10^{-4} M) were dissolved in D_2O and pressurized with H_2 (500 psi) at 20 °C. Under these conditions the butenol was >90% consumed in 1 h (Fig. 6), yielding a turnover frequency of 3000 Rh h^{-1}. Control reactions of the stock solution without catalyst did not yield hydrogenation products.

Increasing the reaction temperature from 20 °C to 45 °C resulted in an increase in the rate of hydrogenation. This result

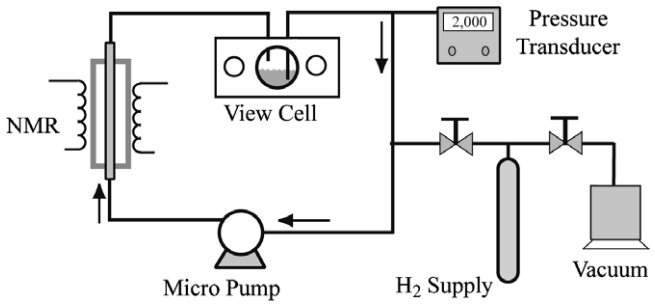

Fig. 5. Flow through NMR set up. All tubing consists of 1/16″ PEEK tubing. The system is capable of flows up to 20 mL/min and allows very efficient mixing.

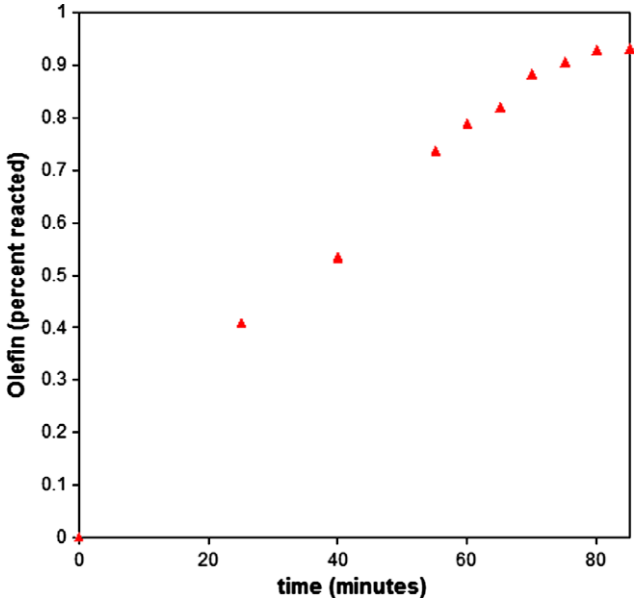

Fig. 6. Catalyst kinetics using the novel flow-through system. At a catalyst concentration of 2.6×10^{-4}, H_2 pressure of 500 psi and butenol concentration of 0.46 M, the catalyst resulted in 3000 turnovers/Rh/h.

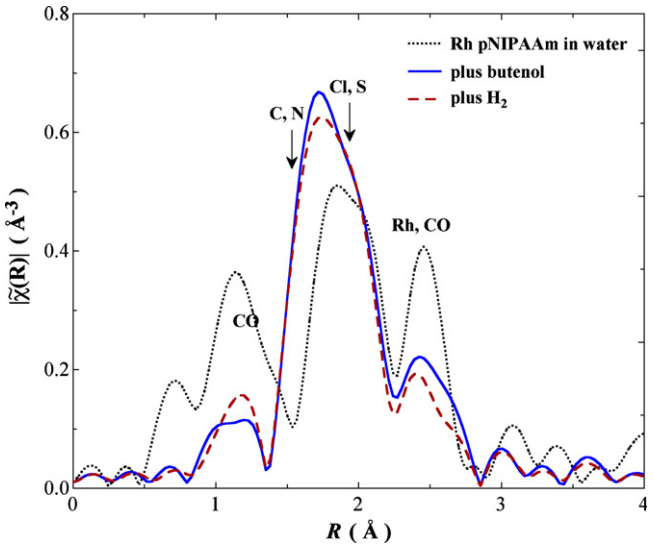

Fig. 7. XAFS RSP data showing the differences in the XAFS spectra as a function of added reagent. In water (black), plus 0.7 M butenol (blue), in water plus 0.7 M butenol and 500 psi H_2 (red). The significant change when in the presence of butenol indicates that butenol in binding. There is no change when H_2 is added, likely due to a very short lifetime for this species. (For interpretation of the references to colour in this figure legend, the reader is referred to the web version of this article.)

was not anticipated due to the expected precipitation of the catalyst complex above the LCST of 33 °C. We found that the LCST of this complex also has a pressure component for which there is literature precedent [29–31]. The filtrate of the hot suspension after depressurization exhibits no color and demonstrates no activity for hydrogenation of butenol. The precipitated solid could be redissolved at room temperature to yield catalytically active solutions. This demonstrates that the catalytic activity resides with the solid and not with a rhodium species free of the polymer. This further demonstrates that the catalyst can be isolated from the product by filtration. This remarkable LCST pressure dependence is the subject of future studies.

The *in situ* catalyst structure was investigated by XAFS (NMR was not used since the COs are unobservable in water). XAFS studies of the active catalyst (4.3 mM) were undertaken in (a) water, (b) water + 0.46 M butenol and (c) water + 0.46 M butenol + 500 psi H_2. The appearance of the solution as prepared in water was very black and gel-like. Investigation of the XAFS spectra revealed no sign of free rhodium metal, which would be readily distinguishable. This indicates that the gel-like phase was due to the high concentration rather than a loss of homogeneous catalyst to rhodium metal. These data are shown in Fig. 7. Specifically of interest was characterizing the ligands in the first ligand sphere to assess if the reactants were binding. In water, the initial ligands are two-CO, one-N, one-Rh and one-S, which then transform to the tetrameric rhodium cluster (Fig. 2a). Upon the addition of butenol, a very substantial change was observed by XAFS, indicating the binding of the butenol to Rh. The data (Table 2) also indicate that the rhodium–rhodium bonds are broken when the butenol is added, as observed before[32], suggesting that the cluster is not critical to the active catalyst species. No significant change occurred in the XAFS upon the addition of H_2.

4. Conclusions

In summary, ^{13}C, ^{15}N and ^{35}Cl NMR, XAFS and FTIR spectroscopic methods were used to resolve the structural details of the evolution of a very active, recoverable polymeric catalyst. The "ligand rearrangement" from NH_2 to SR_2 observed when the solvent conditions are changed from THF to water emphasizes the importance of this kind of characterization in the development of water soluble catalysts. The rhodium–rhodium bonds formed during extended exposure to water are broken when butenol is added during hydrogenation, supporting a very transitional catalyst precursor structure. Hydrogenation kinetics of 3000 turnovers/Rh/h demonstrate this as a promising hydrogenation catalyst. Future work includes investigating the catalytic activity as a function of time to determine if catalytic activity changes significantly with complex transformation.

Acknowledgements

This work was supported by the Laboratory Directed Research and Development Program at the Pacific Northwest National Laboratory operated by Battelle for the U.S. DOE under Contract DE-AC05-76RL01830. The Advanced Photon Source is supported by the U.S. Department of Energy, Office of Basic Energy Sciences, under Contract DE-AC02-06CH11357. PNC-XOR is funded by its founding institutions, the U.S. DOE-BES, and NSERC.

Appendix A. Supplementary material

Supplementary data associated with this article can be found, in the online version, at doi:10.1016/j.jorganchem.2008.03.011.

References

[1] W.J. Shaw, J.C. Linehan, A. Gutowska, D. Newell, T. Bitterwolf, J.L. Fulton, Y. Chen, C.F. Windisch, Inorg. Chem. Commun. 8 (2005) 894.
[2] H.G. Schild, Prog. Polym. Sci. 17 (1992) 163.
[3] D.E. Bergbreiter, B.L. Case, Y.-S. Liu, J.W. Caraway, Macromolecules 31 (1998) 6053.
[4] D.E. Bergbreiter, R. Hughes, J. Besinaiz, C. Li, P.L. Osburn, J. Am. Chem. Soc. 125 (2003) 8244.
[5] D.E. Bergbreiter, Chem. Rev. 102 (2002) 3345.
[6] D.E. Bergbreiter, P.L. Osborn, J.D. Frels, J. Am. Chem. Soc. 123 (2001) 11105.
[7] D.J. Cole-Hamilton, Science 299 (2003) 1702.
[8] T.J. Dickerson, N.N. Reed, K.D. Janda, Chem. Rev. 102 (2002) 3325.
[9] X. Yin, A.S. Hoffman, P.S. Stayton, Biomacromolecules 7 (2006) 1381.
[10] D.N. Lawson, G. Wilkinson, J. Chem. Soc. (1965) 1900.
[11] W. Hieber, H. Lagally, Z. Anorg. Allgem. Chem. 251 (1943) 96.
[12] C.W. Garland, J.R. Wilt, J. Chem. Phys. 36 (1962) 1094.
[13] J.J. Rehr, J.M. d. Leon, S.I. Zabinsky, R.C. Albers, J. Am. Chem. Soc. 113 (1991) 5135.
[14] M. Newville, J. Synchrotron Rad. 8 (2001) 322.
[15] B. Ravel, M. Newville, J. Synchrotron Rad. 12 (2005) 537.
[16] F.A. Cotton, L. Kruczynski, B.L. Shapiro, L.F. Johnson, J. Am. Chem. Soc. 94 (17) (1972) 6191.
[17] W.S. Sheldrick, R. Exner, Inorg. Chim. Acta 195 (1992) 1.
[18] T. Konno, K. Haneishi, M. Hirotsu, T. Yamaguchi, T. Ita, T. Yoshimura, J. Am. Chem. Soc. 125 (2003) 9244.
[19] T. Konno, K.-I. Okamoto, Inorg. Chem. 36 (1997) 1403.
[20] J.R. Dilworth, D. Morales, Y. Zheng, J. Chem. Soc., Dalton Trans. (2000) 3007.
[21] V. Miranda-Soto, J.J. Perez-Torrente, L.A. Oro, F.J. Lahoz, M.L. Martin, M. Parra-Hake, D.B. Grotjahn, Organometallics 25 (2006) 4374.
[22] C. Tejel, B.E. Villarroya, M.A. Ciriano, A.J. Edwards, F.J. Lahoz, L.A. Oro, M. Lanfranchi, A. Tiripicchio, M. Tiripicchio-Camellini, Inorg. Chem. 37 (1998) 3954.
[23] L. Carlton, R. Weber, Inorg. Chem. 35 (1996) 5843.
[24] J. Jazwinski, J. Mol. Struct. 750 (2005) 7.
[25] W. Chen, Y. Xu, S. Liao, Transition Metal Chem. 19 (1994) 418.
[26] D. Dowerah, M.M. Singh, Transition Metal Chem. 1 (1976) 294.
[27] D. Dowerah, M.M. Singh, J. Indian Chem. Soc. LVII (1980) 368.
[28] Z. Nagy-Magos, P. Kvintovics, L. Marko, Transition Metal Chem. 5 (1980) 186.
[29] E. Kato, J. Appl. Polym. Sci. 97 (2005) 405.
[30] F. Meersman, J. Wang, Y. Wu, K. Heremans, Macromolecules 38 (2005) 8923.
[31] K. Otake, R. Karaki, T. Ebina, C. Yokoyama, S. Takahashi, Macromolecules 26 (1993) 2194.
[32] O.S. Alexeev, F. Li, M.D. Amiridis, B.C. Gates, J. Phys. Chem. B 109 (2005) 2338.